NREL
NATIONAL RENEWABLE ENERGY LABORATORY

Electrical Bias as an Alternate Method for Reproducible Measurement of Copper Indium Gallium Diselenide (CIGS) Photovoltaic Modules

Preprint

Chris Deline, Adam Stokes, Timothy J. Silverman, Steve Rummel, Dirk Jordan, and Sarah Kurtz

Presented at SPIE Optics + Photonics 2012
San Diego, California
August 12–16, 2012

Conference Paper
NREL/CP-5200-56078
August 2012

Contract No. DE-AC36-08GO28308

Available electronically at http://www.osti.gov/bridge

Available for a processing fee to U.S. Department of Energy
and its contractors, in paper, from:

U.S. Department of Energy
Office of Scientific and Technical Information
P.O. Box 62
Oak Ridge, TN 37831-0062
phone: 865.576.8401
fax: 865.576.5728
email: mailto:reports@adonis.osti.gov

Available for sale to the public, in paper, from:

U.S. Department of Commerce
National Technical Information Service
5285 Port Royal Road
Springfield, VA 22161
phone: 800.553.6847
fax: 703.605.6900
email: orders@ntis.fedworld.gov
online ordering: http://www.ntis.gov/help/ordermethods.aspx

Cover Photos: (left to right) PIX 16416, PIX 17423, PIX 16560, PIX 17613, PIX 17436, PIX 17721

Printed on paper containing at least 50% wastepaper, including 10% post consumer waste.

Electrical bias as an alternate method for reproducible measurement of copper indium gallium diselenide (CIGS) photovoltaic modules

Chris Deline*, Adam Stokes, Timothy J. Silverman, Steve Rummel, Dirk Jordan, Sarah Kurtz
National Renewable Energy Laboratory, 16253 Denver West Blvd, Golden, CO, USA 80401

ABSTRACT

Light-to-dark metastable changes in thin-film photovoltaic (PV) modules can introduce uncertainty when measuring module performance on indoor flash testing equipment. This study describes a method to stabilize module performance through forward-bias current injection rather than light exposure. Measurements of five pairs of thin-film copper indium gallium diselenide (CIGS) PV modules indicate that forward-bias exposure maintained the PV modules at a stable condition (within 1%) while the unbiased modules degraded in performance by up to 12%. It was also found that modules exposed to forward bias exhibited stable performance within about 3% of their long-term outdoor exposed performance. This carrier-injection method provides a way to reduce uncertainty arising from fast transients in thin-film module performance between the time a module is removed from light exposure and when it is measured indoors, effectively simulating continuous light exposure by injecting minority carriers that behave much as photocarriers do. This investigation also provides insight into the initial light-induced transients of thin-film modules upon outdoor deployment.

Keywords: Thin film, Photovoltaic, Transients, Metastability, CIGS, Forward Bias

1. INTRODUCTION

Changes in the I-V parameters of polycrystalline thin-film PV devices have long been studied, particularly the reversible effect of light exposure and voltage bias on device efficiency[1]. Early on, it was recognized that the open-circuit voltage (V_{oc}) of CIGS and CdTe devices was affected by the prior voltage- and light-exposure history of the device[2, 3]. Because voltage exposure near peak-power voltage (V_{mp}) in the dark resulted in the same reversible increase in V_{oc} and fill factor (FF) as light exposure at V_{mp} bias, it was suggested that these V_{oc} and FF changes are driven by the bias history of the thin-film sample rather than its light exposure history. In these cases, dark storage returns the device's performance to its original value.

Investigation into CIGS device metastability (reversible performance change) has indicated that performance changes can be ascribed in part to intrinsic defect centers functioning as hole traps[4,5]. Biasing the junction shifts the Fermi level, allowing defect states to populate or depopulate. Long characteristic charging times may be due both to the high activation energy of the defect state, and to local atomic displacement and lattice relaxation upon acceptance of charge[6]. First-principles modeling of intrinsic defect states by Lany and Zunger has identified one main complex that could explain the majority of CIGS device metastability: selenium / copper vacancies ($V_{Se} - V_{Cu}$) working in tandem as an amphoteric divacancy complex[7]. This complex behaves as a compensating donor $(V_{Se} - V_{Cu})^{+}$ for Fermi levels near the valence band, and as an acceptor $(V_{Se} - V_{Cu})^{-}$ for higher Fermi levels[8]. In the acceptor configuration, the defect contributes to the net hole density of the absorber[4], which directly increases the V_{oc} and reduces the absorber depletion width, providing additional improvement in V_{oc} and FF from reduced recombination[6]. Removal of bias (either photo-induced or current injected) causes the complex to return to its ground state $(V_{Se} - V_{Cu})^{+}$ in a matter of minutes or hours. Capacitance measurements and other experimental results strongly support the theoretical role of ($V_{Se} - V_{Cu}$) in CIGS device short-term reversible changes[9].

Theoretical calculations have identified a second defect complex that may also contribute to metastable performance of CIGS: indium-on-copper antisite donors (In_{Cu}). Although the defect state is primarily implicated in limiting the V_{oc} of practical CIGS devices due to Fermi-level pinning[10], the deep electron trap state may also contribute to reversible performance changes under specific reverse-bias and red-light exposure conditions[8].

Additional theories on the microscopic processes leading to metastable changes in CIGS performance include ionic drift models, which suggest that the motion of ionic species including indium and copper may be responsible for light-dark performance differences of CIGS devices[11]. It is possible that multiple mechanisms are responsible for device performance changes on different time scales, with longer-term performance change driven by ionic motion rather than reversible population and depopulation of electronic states. However, the evidence of low annual degradation rates on par with that of crystalline silicon modules[12] suggests that long-term degradation of polycrystalline thin-film modules from ionic motion may not be an inherent reliability issue[13]. In fact, the CIGS absorber has been calculated to be quite robust to ionic diffusion / drift, with the electrochemical potential tending to concentrate mobile Cu in the ternary material away from the heterojunction[6].

These longer-term metastable changes pose a challenge when trying to accurately gauge PV module performance following stress testing in module certification tests. The current certification standard for thin-film PV modules—IEC 61646[14] — requires successive light-soaking increments of 43 kWh/m^2 integrated irradiance until the incremental relative changes in measured power are 2% or less. This procedure was designed to account for Staebler-Wronski changes in amorphous silicon modules and is quite likely not optimal for stabilizing polycrystalline CdTe or CIGS PV devices following stress test (damp heat under bias) exposure[15]. For instance, high-temperature exposure typically produces temporary efficiency improvements in a-Si modules that are not replicated in CIGS or CdTe modules.

The challenge of short-term transients is in measuring the performance of thin-film PV devices repeatably under standard test conditions (STC, 1 kW/m^2 irradiance and 25ºC module temperature). A typical approach is to light-expose a particular module that has been stored in the dark prior to measurement. However, to ensure the module is at the requisite 25°C for the performance measurement, the module is typically allowed to cool in the dark for up to 1 hour, which may undo some of the performance changes produced by light exposure.

Our goal is to devise a procedure to maintain the performance of thin-film modules at their outdoor state, so that measurements made either after dark storage, manufacture, or certification will be reproducible, within measurement uncertainty. This procedure is intended to minimize fast transient performance changes that may arise in the few minutes to hours elapsing between light exposure and indoor measurement of a typical CIGS module. Prior reports have dealt with the longer-term performance implications of one-sun light exposure or forward bias in the dark[16,17], but this method deals mainly with performance changes visible in the first several hours of exposure[2,9]. Five pairs of CIGS modules are measured after various sequences of exposures, and the transients are documented and compared with the outdoor-measured performance.

2. METHOD

An investigation of forward-bias exposure on CIGS module performance was conducted with three complementary experiments, some of which shared common exposure steps. The first two studies involved outdoor-deployed CIGS modules, subsequently brought indoors and monitored during dark storage. In Experiment I, five pairs of CIGS modules (commercially available) were allowed to relax from an outdoor-exposed, pseudo-stable condition to an indoor, room-temperature dark state. One of each pair of modules was maintained at I_{mp} forward bias by a power supply, while the other module was maintained unbiased in the dark. The forward-bias operating point of the module was determined by placing a benchtop power supply in constant-current mode, set to the nameplate I_{mp} of the module under test. Both modules were cooled using fans and room-temperature air, which maintained module temperature within several degrees of STC (25 ºC).

Experiment II investigated a single CIGS module as it was repeatedly deployed outdoors with full-sun exposure, then brought indoors, and maintained either at I_{mp} forward bias or unbiased, in the dark at room temperature. Sequentially exposing the same module both with and without bias removes uncertainty from any difference in module response, focusing purely on the difference of one module between forward-bias and no-bias exposure.

Experiment III focused on the transient performance changes of the CIGS modules as they were deployed outdoors and light-exposed under load. The outdoor exposures studied under Experiment III were simply the initial outdoor deployments of Experiment I and II, investigated in more detail. Within the first week of outdoor deployment, normalized I-V curves indicated changes of several percent in V_{oc}, FF, and I_{sc}.

The CIGS modules used in these experiments were obtained from four different manufacturers in five separate batches, labeled here as CIGS A through E. Four of the five pairs of modules (CIGS A, CIGS B, CIGS C, and CIGS E) were of glass-glass monolithic construction, using CIGS active material on a glass substrate construction with a transparent conductive oxide (TCO) layer, an ethylene vinyl acetate (EVA) encapsulant, a glass front sheet, and an aluminum frame. One module group included a weatherproof back sheet as well. CIGS D modules are of a different construction: flexible CIGS cells, tabbed and mechanically integrated into a module with an EVA encapsulant, a backsheet, and a front glass.

The ages of the modules fall into two different groupings. CIGS A modules are of an older vintage constructed in the early 2000s, while CIGS B through CIGS E modules are more modern, obtained after 2009. Additional details are given in Table 1:

Table 1: Module construction and efficiency details

Module group name	Qty	Acquisition year	Construction	Initial area efficiency
CIGS A	2	2003	Framed, monolithic	7.4%
CIGS B	2	2010	Framed, monolithic	11%
CIGS C	2	2011	Framed, monolithic	13%
CIGS D	2	2009	Framed, interconnected cells	8.6%
CIGS E	2	2012	Framed, monolithic	14.5%

2.1 Details for Experiments I and II

Table 2 shows the sequence of Experiment I. A set of two modules from each batch was exposed outdoors at the Outdoor Test Facility (OTF) at the National Renewable Energy Laboratory. The modules were rack mounted at latitude tilt and held at the maximum power point. Temperature- and irradiance-corrected I-V curves were taken every 15 minutes. Outdoor performance curves were collected by a Daystar I-V Multitracer, with plane-of-array irradiance monitored with Kipp & Zonen CMP-11 pyranometers, and back-of-module temperature monitored with a T-type thermocouple. When the maximum power of the modules appeared stable (±2%) the modules were removed from the rack and brought indoors. All modules were light-exposed for at least 30 kWh/m^2.

Within 20 minutes of being brought indoors, an I-V curve was measured for each module on an indoor long-pulse solar simulator (Spi-Sun 4600 SLP). Within 30 seconds, one module was then forward-biased at its nameplate maximum-power current (I_{mp}). The other module was left indoors at open-circuit (unbiased). Both modules were placed in front of fans circulating 25ºC air. I-V sweeps were taken for both modules using the long-pulse solar simulator under Standard Test Conditions (STC) 0.5, 1, 2, 4, 7, 24, and 96 hours after being brought indoors. The biased module was kept under forward bias between measurements and removed from the power supply less than a minute prior to each measurement. The small temperature rise of the forward-biased module (2°–3°C) is accounted for by a temperature correction in the STC measurement. The unbiased module was allowed to relax in the dark between measurements, and is maintained at 25°C.

Table 2: Experiment I sequence

Step	CIGS X module 1	CIGS X module 2
1	Light-exposed 30 kWh/m^2 at MPP I-V curves every 15 minutes	
2	Modules brought indoors Immediate indoor light I-V curve	
3	Dark storage unbiased	Dark storage forward-biased at I_{mp}
	Indoor light I-V curves after 0.5, 1, 2, 4, 7, 24 and 96 hours	

In Experiment II, a single CIGS A module was monitored both outdoors and indoors to determine the reversibility of performance changes in response to light and dark exposure. Table 2 shows the sequence of Experiment II. The experiment is essentially identical to Experiment I, except that rather than testing two modules simultaneously in either a forward-bias or unbiased condition, a single module is tested sequentially in unbiased, then in forward-biased conditions.

Table 3: Experiment II sequence

Step	CIGS A module
1	Light-exposed 30 kWh/m^2 at MPP I-V curves every 15 minutes
2	Module brought indoors Immediate indoor light I-V curve
3	Dark storage **unbiased** Indoor light I-V curves after 0.5, 1, 2, 4, 7, 24 and 96 hours
4	Light-exposed 30 kWh/m^2 at MPP I-V curves every 15 minutes
5	Module brought indoors Immediate indoor light I-V curve
6	Dark storage **forward-biased at I_{mp}** Indoor light I-V curves after 0.5, 1, 2, 4, 7, 24 and 96 hours

The CIGS A module was first exposed outdoors for > 30 kWh/m^2 (step 1) to stabilize its electrical performance. The module was held at P_{mp} during outdoor deployment and characterized by I-V sweeps taken every 15 minutes using the Daystar I-V multitracer, as above. The module was then brought indoors and characterized at STC with a long-pulse solar simulator for up to 96 hours, as above. In steps 4–6 the module was placed back outside for another 30-kWh/m^2 light exposure, then brought back indoors for I-V characterization, again up to 96 hours. This time, the module was placed at I_{mp} forward bias between measurements rather than allowing the module to remain unbiased between measurements.

3. RESULTS AND DISCUSSION

3.1 Experiment I

I-V curves measured after modules were brought indoors indicate a reduction in P_{mp} as the module is stored in the dark without applied bias. Figure 1 shows a series of I-V curves taken for the CIGS A module, which was allowed to relax in the dark without bias. Over the four days of indoor measurement, P_{mp} decreased by ~12%, primarily through loss of V_{oc} and FF.

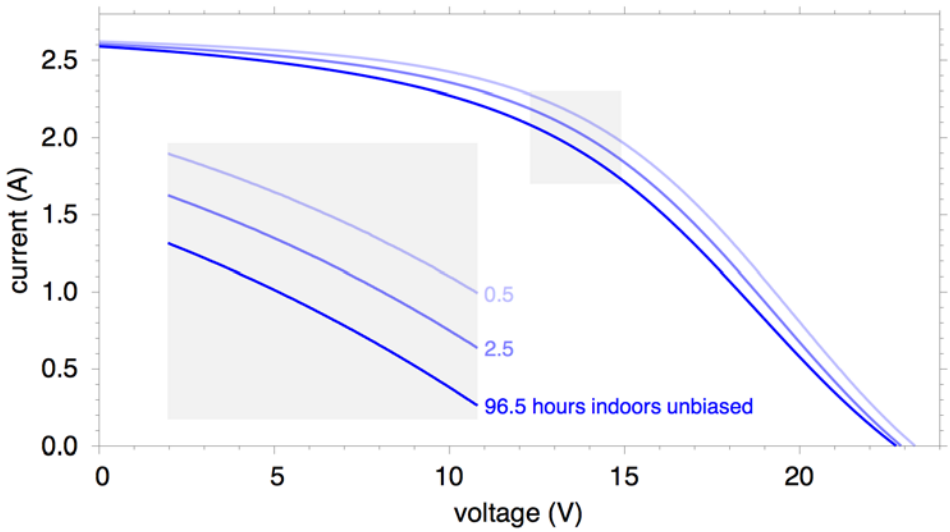

Figure 1: Indoor I-V curves of a CIGS A module, resting in the dark following outdoor exposure. Performance decreased with time as the module rested in the dark at room temperature, particularly through reductions in FF and V_{oc}.

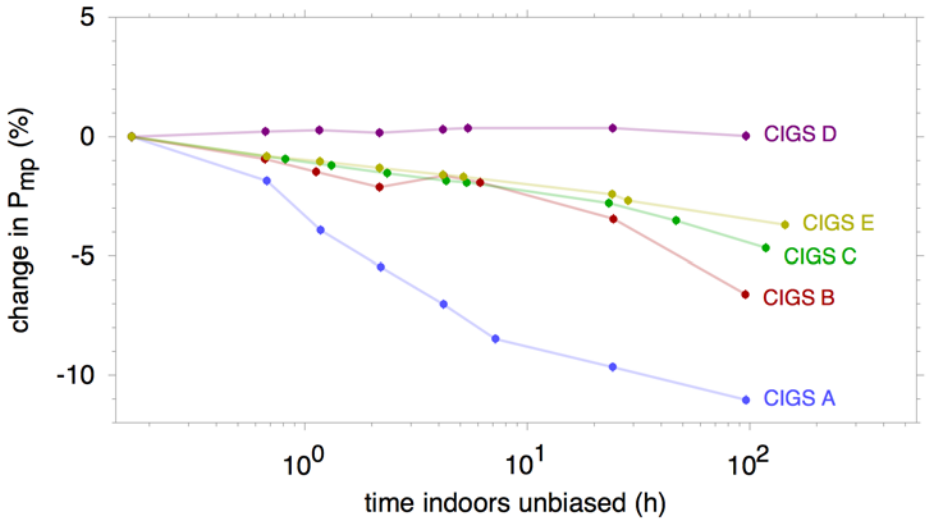

Figure 2: P_{mp} degradation of modules stored in the dark at open-circuit after light exposure. P_{mp} change is calculated as a percentage, relative to the first indoor I-V measurement. CIGS D in particular displayed no measurable change with dark storage. The remaining modules displayed an exponential decay in $\mathbf{P_{mp}}$. Four of the five thin-film models had degraded ~1% or more within one hour.

The reduction in P_{mp} for the other unbiased modules is shown in Figure 2 as a function of time. The performance reduction is displayed as a percentage of the initial indoor I-V measurement point. As was the case in Figure 1, most of the performance change comes from a reduction in V_{oc} and FF, both of which decrease exponentially. In a four-hour span the maximum power degraded 0%–7% depending on the manufacturer. CIGS D, the only module that is not monolithically integrated, was the only module demonstrating little or no change in P_{mp} in response to dark storage. The remaining modules continued to decline in performance up to the end of the measurement period. CIGS A, B, and C did not show an indication of having completely stabilized after 100 hours. However, at the end of the test the reduction in P_{mp} had slowed to approximately 1% every 48 hours.

The early time data in Figure 2 indicate that performance loss due to dark exposure is rapid, with four of the five CIGS modules losing over 1% of P_{mp} within the first hour. It is also evident that the module experiencing the greatest magnitude loss also has the fastest rate of P_{mp} loss (CIGS A in particular). Overall power change after 100 hours in the dark following outdoor light exposure was 0% for CIGS D, –3.7% for CIGS E, –4.7% for CIGS C, –6.6% for CIGS B, and –12.4% for CIGS A. Details are provided in Table 4 showing the P_{mp} loss of each unbiased module following 100 hours of indoor dark storage, along with the rate of each exponential P_{mp} decrease.

Table 4: Performance change and time constant for modules stored in the dark

Module group name	P_{mp} change after 100 hours	Time for half maximum loss
CIGS A	–12.4%	2.5 hours
CIGS B	–6.6%	22 hours
CIGS C	–4.7%	15 hours
CIGS D	0%	N/A (no change)
CIGS E	–3.7%	10 hours

Additional detail on the performance parameters responsible for P_{mp} change for the five unbiased modules is shown in Figure 3, showing that P_{mp} loss is mainly due to FF, with slight reductions in V_{oc}. Again, the CIGS D module showed little change in either V_{oc} or FF. The remaining modules exhibited a fast drop in V_{oc} within the first several hours, quickly stabilizing, except for CIGS B, which sustained V_{oc} loss throughout the entire exposure. Fill factor loss tended to be a more prolonged and sustained decline through the 100-hour dark exposure. I_{sc} (not shown) was relatively constant, increasing slightly (< 0.5%) for most modules.

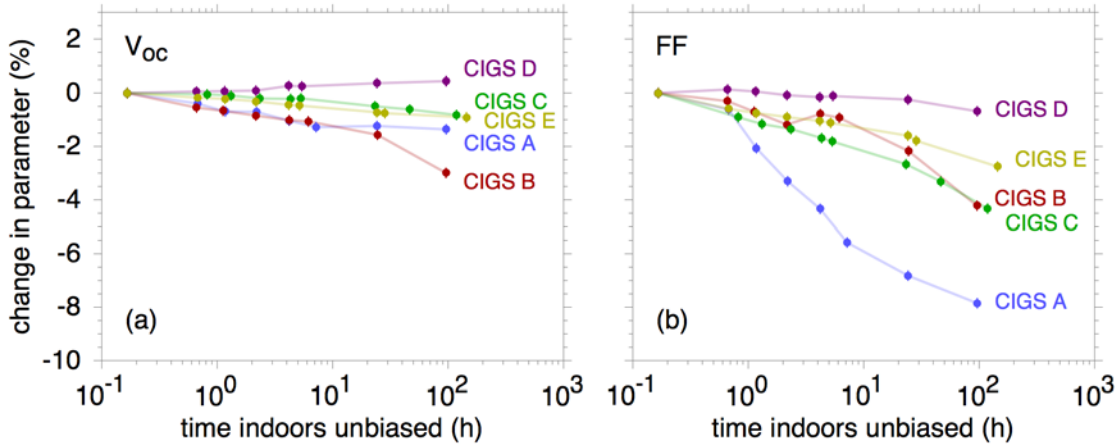

Figure 3: Change in $\mathbf{V_{oc}}$ (left) and FF (right) for the five unbiased modules during dark relaxation, relative to the initial indoor measurement point.

Because of the rapid performance loss experienced by CIGS modules immediately following light exposure, we investigated the possibility of using forward bias to maintain modules at a known performance condition. As the modules shown in Figure 2 were allowed to relax in the dark unbiased, a second module was connected to a power supply at I_{mp} forward bias.

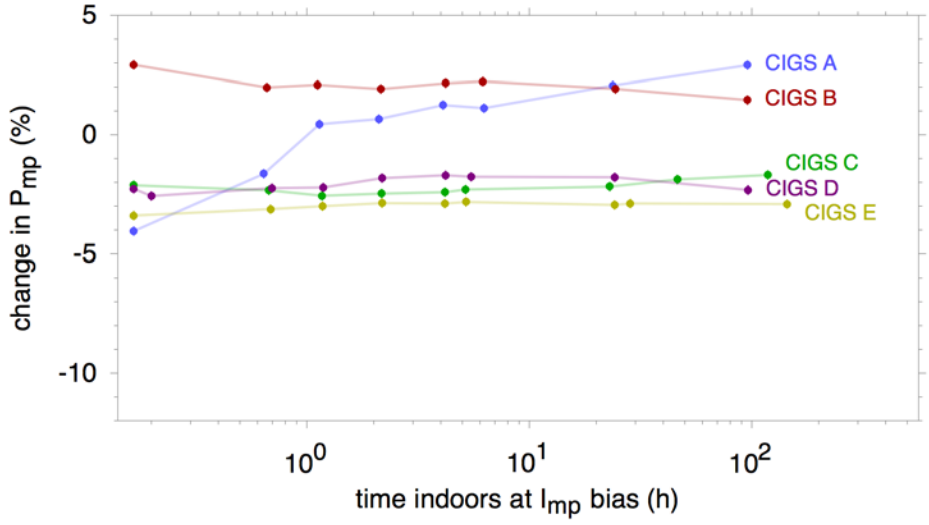

Figure 4: Forward-biased module's $\mathbf{P_{mp}}$ relative to final outdoor performance. In all cases, forward bias results in stabilization of electrical performance to 1%, and final performance within 4% of the outdoor performance of the module.

Figure 4 shows the performance of the second module of each module pair, maintained at I_{mp} bias after being brought indoors. The P_{mp} of each module is measured at the time intervals given in Table 2, and plotted relative to the final outdoor-measured P_{mp} value. Rather than allowing the module's P_{mp} to decline over time, as in Figure 2, the application of forward bias maintains performance within a narrower operating window, especially for module A. Four of the five modules (B through E) have a variation of less than 1% after being brought indoors and measured for the first time.

CIGS C, D, and E are initially measured 2%–3% below their outdoor stabilized condition, and the modules maintain that performance for the next 150 hours. CIGS B is initially measured at 2.5% above its outdoor-stabilized condition, and remains near 1% of that value.

The CIGS A module varied quite rapidly with application of forward bias, increasing in P_{mp} by ~5% within the first hour of biased exposure. In the first hour, CIGS A increased in P_{mp} from 4% below its outdoor-deployed P_{mp} value to 1% above. Additional bias exposure of CIGS A continued a slow P_{mp} increase to a final value 3% above its outdoor deployed P_{mp} value. What is possibly occurring here is that an initial power loss of ~4% might have happened between the final outdoor measurement and the initial indoor I-V measurement as the module was brought indoors. Application of forward bias recovered this transient loss, bringing the final stabilized measurement within a few percent of its long-term outdoor deployed condition.

The reason for CIGS A's large and fast forward-bias response may be connected to the way its twin module performed unbiased. The unbiased module's magnitude of P_{mp} change is the greatest, and the time constant of change is the shortest of all the unbiased modules. A large performance change might occur in both of the CIGS A modules during the short ~20-minute gap between outdoor light exposure and indoor flash testing. This would also indicate that the performance loss shown in Figure 2 for the unbiased CIGS A module may be under-predicting the amount of loss experienced during dark storage. When measuring these CIGS modules, a smaller delay between outdoor light exposure and indoor I-V curve measurement will result in a closer match between the indoor measurement and the long-term outdoor performance.

It should be noted that while four modules stabilized within 1% of their initial indoor-measured condition, the value relative to their final outdoor P_{mp} was either 3% high or 3% low. These modules exhibited stable performance once forward bias was applied, with less than a 1% change throughout the indoor I-V curve measurement. This is notable since the first indoor I-V data point was taken *before* the application of forward bias. Therefore we can say that the bias itself is probably not responsible for the +/– 3% offset value. It is therefore possible that the offset between the indoor and outdoor measured P_{mp} values is a measurement difference between the indoor and outdoor measurement test platforms. A 3% difference between indoor and outdoor STC measurement is within the 5% stated uncertainty in absolute P_{mp} value given for the two testing platforms. Additional uncertainty also arises from the translation equations required to adjust outdoor performance of modules operating at ambient conditions to STC conditions, as will be discussed below.

A clear difference is visible between the modules forward-biased in Figure 4, and their unbiased twins in Figure 2. Except for CIGS D, which did not degrade when left unbiased, the application of bias has clear benefits in terms of the stability of a module's performance, particularly if a module is allowed to wait over an hour between light-soak and measurement. Without bias, the modules experienced between a 1% and 2.5% drop in P_{mp} after an hour in the dark, compared with the forward-biased modules, which maintained stability between 0.5% and 1%, out to 100 hours. Even after 100 hours of resting in the dark, some modules continued to show performance changes, while forward bias appeared to completely stabilize all the modules within a matter of hours.

3.2 Experiment II

The second experiment more clearly shows the advantage of forward-biasing modules prior to indoor measurement by directly comparing results from the same CIGS A module. The module was first light-soaked, then allowed to rest unbiased in the dark between indoor I-V measurements. Then the module was re-deployed outdoors and re-measured indoors, now with I_{mp} bias applied between measurements. Figure 5 shows both the forward-bias and no-bias results for the same CIGS A module.

As in Figure 2 the unbiased CIGS A module rapidly degraded in P_{mp}, losing performance of approximately 14% within the first 24 hours. This performance loss is entirely reversible, with outdoor performance recovering to the same starting value following another 30-kWh/m^2 outdoor light exposure. This time, when the module is placed under I_{mp} forward bias indoors, the performance has an initial drop of 4%–5%, which is recovered within an hour of forward bias. This behavior strongly mirrors the initial loss and subsequent recovery of the forward-biased CIGS A module in Experiment I, as shown in Figure 4. Indeed, the application of forward bias maintains the module at a P_{mp} operating condition within a few percent of the outdoor-deployed value, compared with leaving the module in the dark, which resulted in substantial loss in P_{mp}.

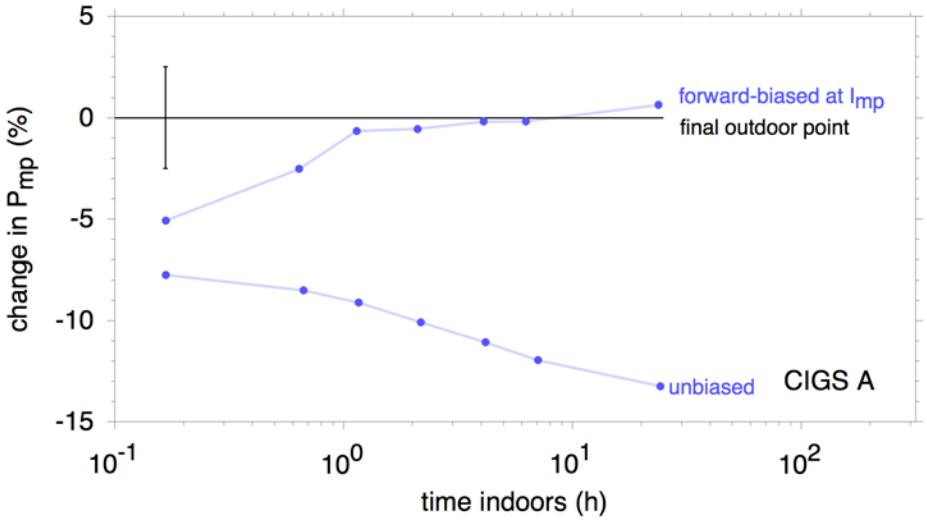

Figure 5: Comparison of the application of forward bias and no bias for the same CIGS A module following light soak. Indoor data is plotted along with P_{mp} from the final stabilized outdoor data.

3.3 Outdoor deployment of modules

I-V data were collected during the outdoor light exposure of the modules and corrected for temperature and irradiance back to STC conditions[18] using manufacturer-provided temperature coefficients. Prior to being deployed outdoors, all modules had been stored in the dark for a period greater than one week.

The outdoor data were first filtered for plane-of-array irradiance between 900 and 1100 W/m^2. Variable conditions were identified that can cause considerable noise in the data. Plane-of-array irradiance was measured before and after the sweep of the I-V curve (taken on the order of several seconds). A change in irradiance of more than 10 W/m^2 during this time period resulted in the rejection of that data point. In addition, it was required that module temperature would change less than 5ºC and irradiance less than 100 W/m^2 in a 5-minute interval. This further reduced the incidence of variable conditions in the outdoor measurements. Additional outliers (caused by partial shading, etc.) can be detected by investigating the ratios of P_{mp} to plane-of-array irradiance and I_{sc} to I_{mp}, which were given acceptance criteria depending on the individual module characteristics.

The data were analyzed for evidence of a recovery in P_{mp} during light exposure, which would indicate the reversibility of P_{mp} losses seen in dark-exposed modules. Figure 6 shows results for one module chosen from each of two module groups: CIGS A and CIGS E. (Outdoor data for CIGS B, C, and D are given in Appendix A.) Individual I-V parameters (P_{mp}, I_{sc}, V_{oc}, and FF) are shown over time after being corrected to initial measured conditions and normalized by module nameplate values.

The largest changes in outdoor performance values were seen in P_{mp} and FF, as was the case with the indoor results. A visible increase in P_{mp} and FF is seen for all modules except CIGS D, which did not experience any change, also in keeping with indoor performance results. To better visualize the changes in P_{mp} and FF, an exponential best-fit line is plotted through the data in Figure 6, according to Eq. 1:

$$F(t) = \theta_1\left[1 - \theta_2 \exp\left(-t/\tau\right)\right] \tag{1}$$

where $F(t)$ is the best-fit function for P_{mp} or FF, θ_1, θ_2 and τ are unconstrained fitting variables, and t is time. This model describes exponential growth with a final value of θ_1. The exponential best-fit is also used to determine the final outdoor-deployed P_{mp} value for the different modules; its value at the conclusion of light soaking is used as an initial reference for the indoor P_{mp} data in Figure 4 and Figure 5.

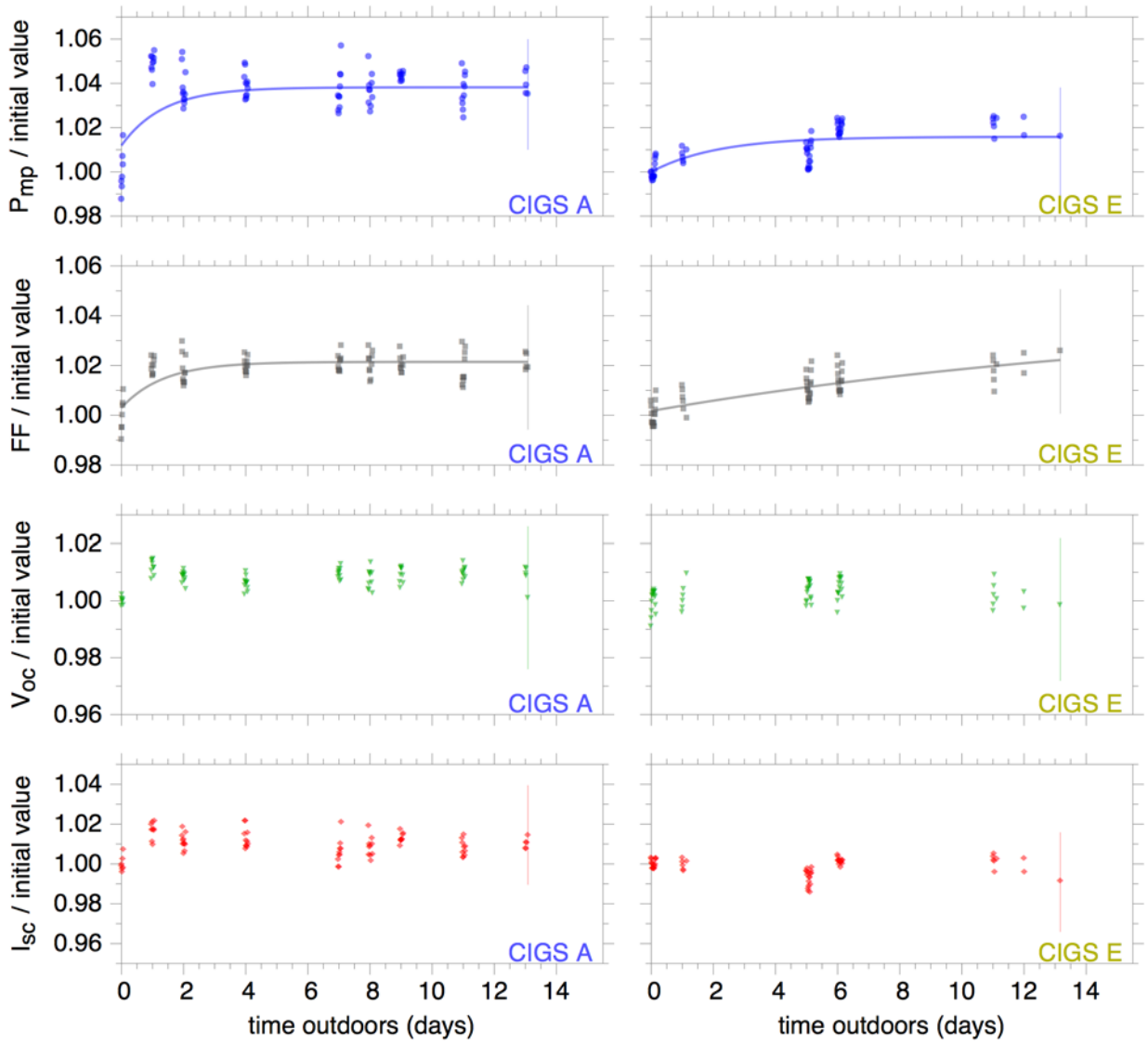

Figure 6: Outdoor I-V parameters for one of the CIGS A modules and one of the CIGS E modules. All performance data are temperature and irradiance corrected and plotted here relative to the module's initial measured value. Uncertainty in outdoor measurement (as indicated by the vertical lines on the right) is on the order of several percent due, in part, to temperature and irradiance corrections. Exponential best-fit to P_{mp} and FF (solid lines) follow Eq. 1.

In the case of the CIGS A and CIGS B modules, outdoor performance stabilizes within the first 2–3 days. For CIGS C and CIGS E modules, stabilization requires more time, roughly one week of outdoor deployment. This is in keeping with the general findings of the indoor measurements that the larger magnitude changes of CIGS A proceeded more rapidly than the smaller magnitude changes of CIGS C and CIGS E. Although these modules were all deployed outdoors during initially sunny conditions, several gaps exist in the plots of Figure 6, generally indicating variable or cloudy conditions. Also, ambient temperature was different for the exposure of various modules, with CIGS A-C deployed in December and February, and CIGS D and CIGS E deployed in March and May. It is unclear how different irradiance or ambient temperature conditions affected the rate of outdoor stabilization of these modules.

The rate of change for outdoor light-exposed modules was different from the indoor decay of P_{mp} in the dark. For CIGS A and B, the outdoor-exposed modules reached a stable condition after being deployed outdoors for 1–3 days. However, no such stabilization was seen in a similar time interval of indoor dark storage. Both CIGS A and CIGS B maintained a downward trend in performance over 100 hours of indoor storage. Conversely, for CIGS C and CIGS E modules, the outdoor performance data showed that stabilization—if achieved at all— required over a week of outdoor exposure, but the indoor dark-exposed modules reached a P_{mp} minimum within several days of dark storage.

3.4 Comparison with theory

As mentioned in the introduction, reversible performance loss in CIGS modules has been studied previously, with several possible mechanisms identified to explain the dark/light metastability. In this experiment, the primary I-V parameter lost during indoor dark exposure was FF, followed by V_{oc}. Timescales for this performance loss range from an hour to > 100 hours, depending on module vintage and construction. It is possible that the performance loss is consistent with the Lany-Zunger defect mechanism, which primarily affects V_{oc}, and secondarily FF. However, not all CIGS modules exhibited loss in V_{oc} and FF. Notably, the CIGS D module exhibited a small V_{oc} increase in response to dark exposure instead of a decrease. More work must be done to identify the reasons for this difference in behavior, and to determine whether it is related to the tabbed-cell module construction of CIGS D (as opposed to monolithic construction), or if the difference is attributable to the active layer of the CIGS D modules. Regardless of the cause of the reversible P_{mp} loss in the dark, it has been shown here that the application of I_{mp} forward bias to CIGS modules stored in the dark will maintain CIGS module performance near outdoor light-exposed performance. The impact of dark storage P_{mp} loss can be mitigated by this procedure, which may allow for more accurate indoor I-V measurements of thin-film modules without the need for costly or bulky indoor light-soaking equipment.

4. CONCLUSION

We have documented the reversible performance change of five pairs of CIGS PV modules in response to outdoor light exposure and indoor dark storage. We identified that in four of the five modules, dark exposure led to a loss in P_{mp} between 3% and 12%, driven largely by FF and V_{oc} reduction, consistent with the metastability mechanism proposed by Lany and Zunger. Time scales for this performance loss are on the order of hours to tens of hours, highlighting the importance of quick measurement of CIGS modules following light exposure, if thin-film modules are to be measured on indoor flash-test equipment.

An alternative to light exposure of CIGS modules prior to indoor measurement was investigated by applying forward bias to each module. The constant current of this forward bias was set to the nameplate rated I_{mp} of each module. Stabilization of each module was accomplished by less than an hour of forward bias, after which the module's performance varied less than 1%, for the entire 100-hour experiment. The stabilized P_{mp} of the modules under forward bias was within 3% of the final outdoor-deployed P_{mp} measurement. More work is needed to determine whether the 3% difference reflects the uncertainties from outdoor measurement and translation to STC or a difference in the mechanism underlying the observed transients.

Application of forward bias to CIGS modules brought indoors enables the collection of indoor I-V measurements that may be closer to the long-term outdoor measurements than when modules are stored unbiased. This relieves the time pressure of staging the modules in the solar simulator immediately after they are brought indoors. Furthermore, the method reduces variability in measurements that are taken on the same module or type of module, but with different delays between the light exposure and the moment the measurement is made.

ACKNOWLEDGEMENT

We thank Alan Anderberg from the NREL Cell and Module Characterization Team for measurements performed at STC. This work was supported by the U.S. Department of Energy under Contract No. DOE-AC36-08GO28308 with the National Renewable Energy Laboratory.

REFERENCES

[1] Gostein, M. and Dunn, L., "Light Soaking Effects on Photovoltaic Modules: Overview and Literature Review," *Proc. 37th IEEE PVSC*, Seattle, WA, June 19-24, 2011.

[2] Sasala, R.A. and Sites, J.R., "Time dependent voltage in CuInSe2 and CdTe solar cells," *Proc. 23rd IEEE PVSC*, pp. 543-548 (1993).

[3] Ruberto, M.N. and Rothwarf, A., "Time-dependent open-circuit voltage in $CuInSe_2$/CdS solar cells: Theory and experiment," *J. Appl. Phys.* **61**, 4662 (1987).

[4] Engelhardt, F. et al., "Metastable electrical transport in Cu(In,Ga)Se_2 thin films and ZnO/CdS/Cu(In,Ga)Se_2 heterostructures," *Physics Letters A* **245**, pp. 489-493 (1998).

[5] Igalson, M. and Schock, H.-W. *J. Appl. Phys.* **80**, 5765 (1996).

[6] Guillemoles, J., Kronik, L., Cahen, D., Rau, U., Jasenek, A., Schock, H., "Stability Issues of Cu(In,Ga)Se_2 –Based Solar Cells," *J. Phys. Chem. B* **104**, pp. 4849-4862 (2000).

[7] Lany, S. and Zunger, S., "Light- and bias-induced metastabilities in Cu(In,Ga)Se_2 based solar cells caused by the (V_{Se}-V_{Cu}) vacancy complex," *Journal of Applied Physics* **100**, p. 113725 (2006).

[8] Siebentritt, S. Igalson, M., Persson, C., Lany, S., "The electronic structure of chalcopyrites – bands, point defects and grain boundaries," *Progress in Photovoltaics* **18**, pp. 390-410 (2010).

[9] Igalson, M, Cwil, M., Edoff, M., "Metastabilities in the electrical characteristics of CIGS devices: Experimental results vs theoretical predictions," *Thin Solid Films* **515**, 6142-6146 (2007).

[10] Lany, S. and Zunger, A., "Intrinsic *DX* centers in Ternary Chalcopyrite Semiconductors," *Physical Review Letters* **100**, 016401 (2008).

[11] Loef, R., Schoonman, J., Goossens, A., "Investigation of capacitance transients in $CuInS_2$ due to ionic migration," *Solar Energy Materials & Solar Cells* **92**, 1579-1585 (2008).

[12] Jordan, D. and Kurtz, S., "Thin-film reliability trends toward improved stability," *Proc. 37th IEEE PVSC*, Seattle, WA, pp. 000827-000832 (2011).

[13] Rau, U., Jasenek, A., Herberholz, R., Schock, R., Guillemoles, J.-F., Lincot, D., Kronink, L. "The inherent stability of Cu(In,Ga)Se2-based solar cells," *Proc. 2nd WCPEC*, Vienna, 428-433 (1998).

[14] IEC 61646, "International Standard: Thin-film terrestrial photovoltaic (PV) modules – Design qualification and type approval," Sec. 10.19; International Electrotechnical Commission Central Office 3, rue de Varembé, CH-1211 Geneva 20 Switzerland, 2nd ed. (2008).

[15] Sample, T., "Preconditioning of Thin-Film PV Modules Through Controlled Light-Soaking," *NREL Photovoltaic Module Reliability Workshop*, Golden, CO, 2012, available online at http://www1.eere.energy.gov/solar/pdfs/pvmrw12_thuram_sample.pdf.

[16] del Cueto, J.A., Deline, C.A., Rummel, S.R., Anderberg, A. "Progress toward a stabilization and preconditioning protocol for polycrystalline thin-film photovoltaic modules," *Proc. 35th IEEE PVSC* (2010).

[17] Deline, C., del Cueto, J., Albin, D., Rummel, S., "Metastable electrical characteristics of polycrystalline thin-film photovoltaic modules upon exposure and stabilization," *J. Photon. Energy* **2**, 022001 (2012), DOI:10.1117/1.JPE.2.022001.

[18] Marion, B., "Comparison of Predictive Models for Photovoltaic Module Performance," Equation (2), *Proc. 33rd IEEE PVSC*, San Diego, CA (2008).

APPENDIX A: OUTDOOR DATA FOR CIGS B-D